CRYSTAL GROWTH & DESIGN
2008
VOL. 8, NO. 7
2335–2339

Studies on the Growth, Optical, Thermal, and Mechanical Properties of Pure and *o*-Nitroaniline Doped Benzil Crystals

T. Kanagasekaran, P. Mythili, P. Srinivasan, Ahmad Y. Nooraldeen, P. K. Palanisamy, and R. Gopalakrishnan*

Department of Physics, Anna University, Chennai-600 025, India

Received November 17, 2007; Revised Manuscript Received January 2, 2008

ABSTRACT: Pure and *o*-nitroaniline (O-NA) doped benzil single crystals were grown by the slow cooling solution growth method. The doping of O-NA is associated with the strong interaction between the guest and host molecules by the hydrogen bonding. Incorporation of O-NA in the lattice enhances the crystallinity. The nonlinearity increases due to the inductive nitro group added to the benzil. The values of nonlinear absorption coefficient (β) and nonlinear refractive index (n_2) of benzil are -78×10^{-3} cm/W and -22×10^{-3} cm/W, while the corresponding values for O-NA doped benzil are -9.4×10^{-9} and -6×10^{-7} cm^2/W, respectively. The figure of merit values of benzil and O-NA doped benzil are 2265 and 4990, respectively. The increase in hardness on doping of O-NA to benzil is due to the strong hydrogen bond.

1. Introduction

Organic molecular materials are attractive in controlling a light beam by an electric field because they offer many possibilities to tune their optical properties and obtain large electro-optic effects.[1] These materials are interesting in the design of the interfaces between the optical and the electrical communication network, and investigation of their intrinsic properties have become very important assuming a microscopic origin for any change in macroscopic properties.[1] Optical materials with large nonlinear refractive index (γ) and nonlinear absorption coefficient (β) values are promising materials for nonlinear optical (NLO) devices such as ultrafast optical switches and power limiters, because of their high durability and the ease of fabricating waveguides and fibers. Negative γ induces self-focusing of an irradiation beam in a material. Since the absolute magnitude of negative γ (at high frequencies) is often larger than that of positive γ (at low frequencies) for a given material,[2] devices with negative γ can be operated at smaller input power. Therefore, negative γ is expected to give devices a longer lifetime. Many optical materials such as oxide crystals[3] and oxide glasses have positive γ, but negative γ in the wavelength range of visible light (under pulsed laser excitation) has been reported only for a few semiconductors and semiconductor-doped glasses.[4] Benzil, a semiconducting material, is also reported to have ferroelectric nature.[1] Therefore, it is interesting to tailor this material with negative γ.

The benzil molecule has a skew structure in which two benzoyl units (C_6H_5-CO) are planar forming a dihedral angle of approximately 90°. The dicarbonyl system (O═) C−C (═O) is non-coplanar and the twist angle between the two carbonyl groups is 111° in the ground-state in the solid state. The ferroelectric behavior of benzil is associated with a second-order phase transition at low temperature that converts the room temperature uniaxial form to a low temperature biaxial form with effects on the phase matching process for an efficient optical nonlinear phenomenon and subsequent significant electro-optic effect.

o-Nitroaniline is more easily reduced than para. This behavior is due to the effect of hydrogen bonding involving the nitro and amino groups. The tendency to decrease the resonance energy of the conjugated system involving the nitro group and *o*-amino group through electrostatic attraction between induced terminal charges tends to make the nitro group more easily reduced. In general, the strength of an unsymmetrical hydrogen bond D−H···A is increased by increasing the resultant positive charge of D and the negative charge of A. This was shown for *o*-nitroaniline.[5] It was also reported by Rai et al.[6] that the binary compound of *m*-nitroaniline (m-NA) and benzil exhibits less NLO behavior, which led us to probe the cause for it and further enhance the NLO behavior of benzil. When the O-NA is doped with benzil, the lone pair of electrons in the carbonyl group of benzil forms the hydrogen bond. Hence, in the present investigation a systematic study on O-NA doped benzil has been made, and the growth, optical, thermal, and mechanical properties of benzil and O-NA doped benzil single crystals are reported.

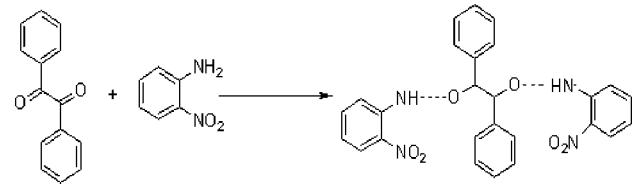

Figure 1. Reaction scheme of O-NA doped in benzil.

2. Experimental Procedures

Benzil and O-NA doped benzil single crystals were grown by the slow cooling solution growth technique. On the basis of the solubility and nucleation studies carried out on benzil, acetone was chosen as the solvent for the growth of benzil and O-NA doped benzil crystals. 0.5 mol% of O-NA was added in the saturated solution of benzil. The possible reaction scheme is depicted in Figure 1. The material was purified by the recrystallization process, using acetone as the solvent. Single crystals of benzil and O-NA doped benzil were grown from saturated solution at 40 °C using a constant temperature bath with a control accuracy of ±0.01 °C. Figure 2 shows the grown single crystals of benzil and O-NA doped benzil.

The UV−vis spectra of benzil and O-NA doped benzil crystals were recorded in the wavelength range of 200 and 1200 nm using a Varian Cary 5E UV−vis-NIR spectrometer. The photoluminescence (PL) spectra were recorded using a home assembled PL system at National Physical Laboratory (NPL), New Delhi, consisting of a two-stage

* Corresponding author: E-mail: krgkrishnan@annauniv.edu, krgkrishnan@yahoo.com. Tel: +91-44-22203374. Fax: +91-44-22203160.

10.1021/cg701132f CCC: $40.75
Published on Web 05/28/2008

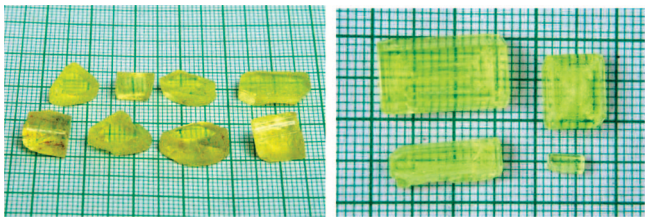

Figure 2. As-grown crystals of benzil and O-NA doped benzil.

monochromator, a photomultiplier tube (PMT) with a lock-in amplifier for PL detection, and an Ar^+ ion laser operating at 488 nm and 5 mW (corresponding to 0.125 W cm^{-2}) for excitation in all the measurements. Vickers microhardness tester (mhp-100) equipped with a diamond pyramid indenter attached to an incident-light microscope (Neophat-2; Carl Zeiss, Germany) was used for measuring the mechanical hardness of the benzil and O-NA doped benzil crystals. The second harmonic generation (SHG) efficiency was measured using the Kurtz-Perry powder technique. The nonlinear refractive index and nonlinear absorption coefficient of benzil and O-NA doped benzil were calculated by means of the Z-scan technique. The Z-scan experiments were performed using a 532 nm diode-pumped Nd: YAG cw laser beam (Coherent Compass TM 215M-50). The lens with the focal length of 3.5 cm was used. The radius of the focused beam waist in the sample was equal to ~70 μm approximately. The diameter of the aperture placed at a distance of 70 cm from the focal waist of the beams was equal to 2.5 mm. The crystal sample of 1 mm thickness was cut from the bulk crystal. The thickness of the crystal is considerably less than the diffraction length of the used focused laser beam, that is, the thin sample approximation of the Z-scan method is fulfilled ($Z_R = 2.9$ mm). The schematic diagram of the experimental setup used is shown in Figure 3. The transmission of the beam through an aperture placed in the far field was measured using photodetector fed to the digital power meter (Field master Gs-coherent). For an open aperture Z-scan, a lens to collect the entire laser beam transmitted through the sample replaced the aperture. The experiments were performed at room temperature.

3. Results and Discussion

3.1. X-ray Diffraction. The single crystal X-ray diffraction (XRD) data of the grown O-NA doped benzil crystals were obtained using a single crystal X-ray diffractometer (model: ENRAF NONIUS CAD4), and the crystallographic data are given in Table 1. From the single crystal XRD analysis, it is confirmed that the grown crystal is hexagonal and the space group is $P3_121$. The obtained crystallographic data reveal that there is a variation in the lattice parameters indicating the presence of the dopant.

3.2. Fourier Transform-Infrared Spectrum. The Fourier transform infrared spectrum of O-NA doped benzil is shown in Figure 3. The band at 1660.6 cm^{-1} is assigned to the symmetric C═O stretch of the diketo group and N−H plane bending mode of O-NA. The doped O-NA in benzil is evidenced from the C−N stretch at 1095.5 and 1072.3 cm^{-1}, while the band at 1170.7 cm^{-1} is attributed to the phenyl-C stretch in aromatic ketones. The aromatic C−H stretch is found at 3058.9 cm^{-1}. The band at 1503 cm^{-1} is due to vibrations of the aromatic ring and the band at 1014 cm^{-1} is due to the symmetric C−O stretch. The formation of the hydrogen bonding is ascertained by the O−H stretching at 3307.4 cm^{-1}. The C−N stretch of the NO_2 group is found at 866 cm^{-1}. Also the benzil units are found at 688.5 and 640.3 cm^{-1}.[7]

3.3. UV−visible Spectral Analysis. The peaks observed in the absorption spectra of the benzil crystals cannot be attributed to the excitons. This peak is correlated with some particularities of the molecular confirmation being assigned to dicarbonyl group absorption in benzil. The presence of lone electron pairs of O atoms in carbonyl groups in benzil (designed nonbonding e^-s) is favorable to the promotion of an electron to an unoccupied π^* orbital giving an (n, π^*) excited state. In the solid state some of the carbonyl groups are close to one another and because of the strong interaction between their electrons it is expected to split into two bonds of the n-π^* level in dicarbonyls. The absorption edge process in benzil is correlated with absorption bands corresponding to the two compounds obtained by the split of the n-π^* state. The band of the (n, π^*) level is assumed to be the origin of absorption edge in benzil with energetic thresholds at $E_g = 2.71$ eV. The effect of impurities on the shape and position of the emission peaks in benzil has been investigated, and no significant shift of the absorption peak situated at 2.71 eV is observed. The most important feature of the fundamental light absorption in benzil is that the existence of the absorption is unchanged in benzil doped with O-NA. The spectrum of the pure benzil crystal is shown in Figure 4a. The crystal has a strong absorption below 450 nm and is almost clear in the near-infrared (IR) range of the spectrum. This makes the host material potentially suitable for laser applications in the near IR region. The absorption spectrum of O-NA doped benzil is shown, and the main absorption peaks are identified in Figure 4b.[8] The change in the color of the crystal from light yellow to greenish yellow on addition of O-NA could explain the donor−acceptor complex formation. The doping of O-NA induces significant changes in the spectrum of benzil. This could be associated with the weak van der Waals bond, and the stronger interaction, that exists between the guest and host molecules by the hydrogen bonding.

3.4. Photoluminescence (PL) Studies. Defects have serious implications on luminescence materials as they provide nonradiative recombination routes for electrons and holes. In order to have a material to be as efficient as possible, the number of electron/hole recombinations via optically active centers must be maximized. Higher PL intensity can be obtained as a result of the improved crystal quality.[9] We observe a weak shoulder at 2.34 and 2.14 eV corresponding to pure and O-NA doped benzil, respectively (Figure 5a,b). Luminescence spectra in benzil doped with O-NA shows a sharp peak at 2.14 eV, which can be associated with the impurities (O-NA). However, the intensity of the peak is increased on doping with O-NA. This corresponds to the yellow luminescence. Yellow luminescence is caused by electron recombination between the shallow donors and acceptors in the conduction band. Yellow luminescence originates from extended defects inside grains and at low-angle grain boundaries. Also yellow luminescence can be attributed to the shallow donor−acceptor transitions.[10] The increase in the intensity of the peak is measured as the ratio of the intensity of the doped benzil crystal to the intensity of the pure benzil crystal. The intensity of the peak increases up to 17.36 times on doping with O-NA to benzil. The PL intensity is highly dependent on the crystallinity, surface morphology, and composition of the ratio of the dopant.

3.5. Nonlinear Optical Characterization. 3.5.1. Kurtz-Perry Powder Technique. The grown crystals were characterized for their NLO property. For this purpose, the output from Nd:YAG laser (1064 nm) model GCR-2 (10) was focused on the powdered benzil and O-NA doped benzil. We have carried out the Kurtz-Perry experiments with the identical particle size sieved in a sieving plate containing the particle size of 125−150 μm. Pulse energy was 5 mJ/s and pulse width was about 10 ns. The output could be seen as a bright green flash emission from the benzil and O-NA doped benzil samples. The SHG of benzil and O-NA doped benzil were compared with that of KDP. It was found that the SHG output of KDP resulted in a 240 mV

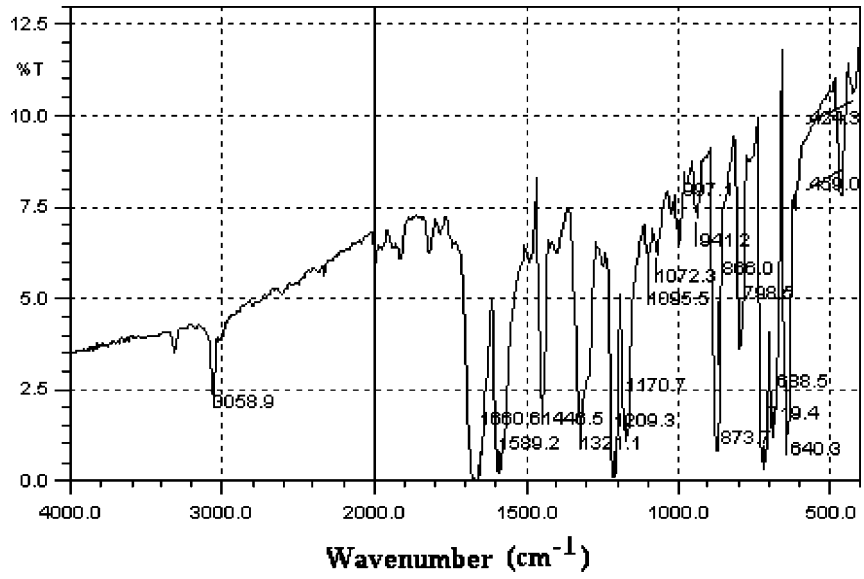

Figure 3. FTIR spectrum of O-NA doped benzil.

Table 1. Lattice Parameters of Benzil and O-NA Doped Benzil

sample	*a*, Å	*b*, Å	*c*, Å	α	*β*	*γ*	volume, Å^3
benzil	8.412(4)	8.412(4)	13.655(9)	90.00(9)°	90.00(8)°	120(1)°	966.25
O-NA doped benzil	8.423(4)	8.423(4)	13.888(9)	*90.00(9)°*	*90.00(8)°*	*120(1)°*	985.31

signal in the photodetector. While benzil gave a 1.2 V signal, O-NA doped benzil gave a 2.4 V signal at given pulse energy of 5 mJ/s, when the output of KDP was 240 mV. Benzil is a molecule of high optical polarizability and has a relatively high dipole moment. When a polarizable and highly inductive substituent group, such as a nitro group, is coupled to the polarizable aromatic nucleus the nonlinear coefficient increases.[11] Hence, with the addition of O-NA to benzil second-order nonlinearity increases.

3.5.2. Z-Scan Studies. Sheik-Bahae et al. have presented a simple but sensitive single beam technique called Z-scan for determining both the magnitude and sign of nonlinear refractive index (γ) and nonlinear absorption coefficient (β).[12] Nonlinear refractive index and nonlinear absorption of benzil and O-NA doped benzil crystals (thickness $\approx$ 1 mm) were studied using the single-beam Z-scan technique with CW laser at 532 nm (SHG diode pumped Nd:YAG laser). The study of nonlinear refraction by the Z-scan method is based on its dependence on the position Z, of the investigated thin samples along a focused Gaussian laser beam. The sample causes an additional focusing or defocusing, depending on whether nonlinear refraction is positive or negative. As a result, the power of the beam passing through a small aperture placed in the far field is varied when moving the sample along Z. It is named as the closed-aperture Z-scan. The "peak-valley" or "valley-peak" dependences of the beam transmittance versus Z are obtained.[13] The experimental set up is shown in Figure 6.

When the aperture is absent (open-aperture Z-scan) the changes in the measured signal during the Z-scan is due to nonlinear absorption. Nonlinear refraction does not affect the

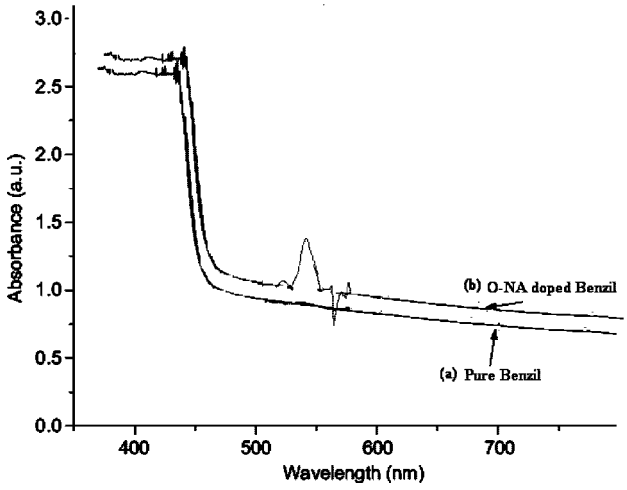

Figure 4. UV−visible spectrum of (a) benzil and (b) O-NA doped benzil.

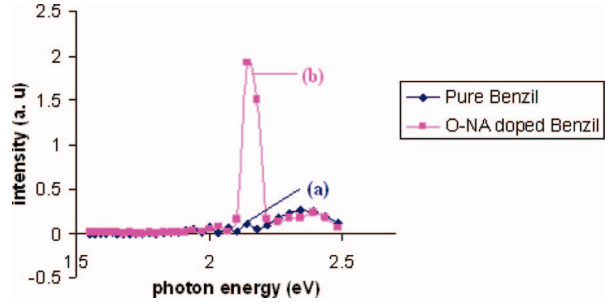

Figure 5. Photoluminescence spectrum of (a) benzil and (b) O-NA doped benzil.

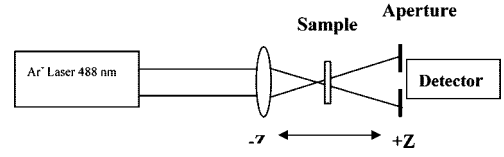

Figure 6. Experimental set up for the Z-scan technique.

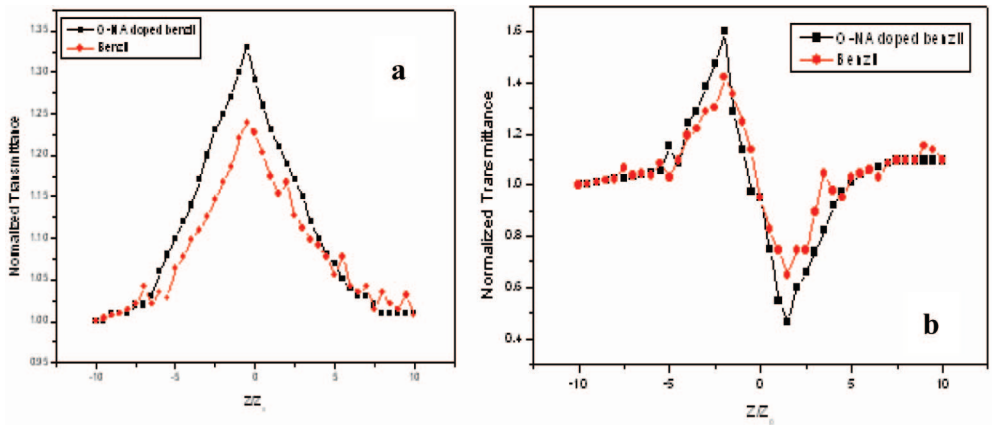

Figure 7. Z-scan technique for (a) open aperture and (b) closed aperture for benzil and O-NA doped benzil.

whole integrated signal in this case. The pure nonlinear refraction in the sample is determined by taking the ratio of the closed Z-scan signal to the open Z-scan signal.

A typical closed-aperture Z-scan of the benzil and O-NA doped benzil showing the normalized transmittance for incident intensity $I_o = 0.303$ kW/cm^2 is shown in Figure 7b. The curves are characterized by a prefocal peak followed by a postfocal valley, which implies that the nonlinear refractive index of the crystal is negative ($n_2 < 0$). Figure 7a shows the typical Z-scan data for the open aperture for benzil and O-NA doped benzil. The nonlinear refractive index (n_2) was calculated using the standard relations[14,15]

$$\Delta T_{P-v} = 0.406(1 - S)0.25^*/\Delta\Phi\circ \quad (1)$$

where ΔT_{P-v} can be defined as the difference between the normalized peak and valley transmittance, $T_{P-v}/\Delta\Phi^\circ$ is the on-axis phase shift at the focus, S is the linear transmittance of the aperture, and nonlinear refractive index can be given by

$$n_2 \approx \frac{\Delta\varphi_o}{kI_oL_{eff}} \quad (2)$$

$$\beta = \frac{2\sqrt{2}\Delta T}{I_oL_{eff}} \quad (3)$$

where n_2 is the nonlinear refractive index, β is the nonlinear absorption coefficient, k is the wavenumber ($k = 2\pi/\lambda$), and $L_{eff} = (1 - e^{-\alpha L})/\alpha$ with $I_o = 2P/\pi w_o^2$ defined as the peak intensity within the sample, where L is the thickness of the sample, and α is the linear absorption coefficient. Using the ratio of the signals with and without the aperture accounts for the nonlinear absorption and gives the information about purely nonlinear refraction. The enhanced transmission near the focus is indicative of the saturation of absorption at high intensity. Absorption saturation in the sample enhances the peak and decreases the valley in the closed aperture Z-scan. The defocusing effect is attributed to a thermal nonlinearity resulting from absorption of radiation at 532 nm. Localized absorption of a tightly focused beam propagating through an absorbing medium produces a spatial distribution of temperature in the crystal and, consequently, a spatial variation of the refractive index that acts as a thermal lens resulting in phase distortion of the propagating beam. The values of nonlinear refractive index n_2 of benzil and O-NA doped benzil are -9.4×10^{-9} and -6×10^{-7} cm^2/W, respectively, and from the open Z-scan curve the estimated values of nonlinear absorption coefficient β of benzil and O-NA doped benzil are -78×10^{-3} cm/W and -22×10^{-3} cm/W, respectively. The large nonlinear refraction with high nonlinear figure of merit (FOM) is an ideal property of materials for nonlinear applications including optical power limiters. The FOM is calculated by using the following equation.[16]

$$\text{figure of merit} = \frac{n_2}{\beta\lambda} \quad (4)$$

FOM values of benzil and O-NA doped benzil are 2265 and 4990, respectively. This implies that the FOM increases on doping of O-NA with benzil, which confirms that the addition of O-NA increases the nonlinearity of the benzil, hence making it highly useful for NLO applications.

3.6. Thermal Analysis. The thermogravimetric analysis of O-NA doped benzil was carried out between 30 and 600 °C. The resulting DTA/TGA trace is shown in Figure 8. The melting point of benzil is 95 °C, but when the O-NA is doped with benzil, the melting point is 100 °C. There is a major weight loss at about 242.8 °C. It leads to 51% weight loss up to 320 °C and 61% weight loss up to 600 °C. This corresponds to decomposition of the sample. The crystal lattice is devoid of any water, as there is no loss below 150 °C in the DTA trace.

3.7. Microhardness Analysis. 3.7.1. Load Dependence of Hardness. The indentation marks were made on the (001) plane of O-NA doped benzil single crystals using Vicker's microhardness tester. Figure 9 shows the plot of variation of hardness number with load for pure and O-NA doped benzil. As the load increases the hardness value increases. Here both the pure and O-NA doped benzil exhibit the reverse indentation size effect. The hardness value of O-NA doped benzil is found to be higher than pure benzil. The increase in hardness on O-NA doped benzil may be due to strong hydrogen bond formation with dopant. In the case of the reverse indentation size effect (ISE),[17] a specimen does not offer resistance or undergo elastic recovery, but undergoes relaxation involving a release of the indentation stress away from the indentation site. This leads to a larger indentation size and hence to a lower hardness at low loads. Examination of the indented surfaces of pure and O-NA doped benzil samples reveals the appearance of cracks around indentations when $P \geq 40$ g. Such cracks are typical for brittle materials.

4. Conclusions

The benzil and O-NA doped benzil crystals were grown by the slow cooling method. The grown O-NA doped benzil was confirmed by the single X-ray diffraction and FTIR spectrum. The UV−visible studies show the doping of O-NA induced

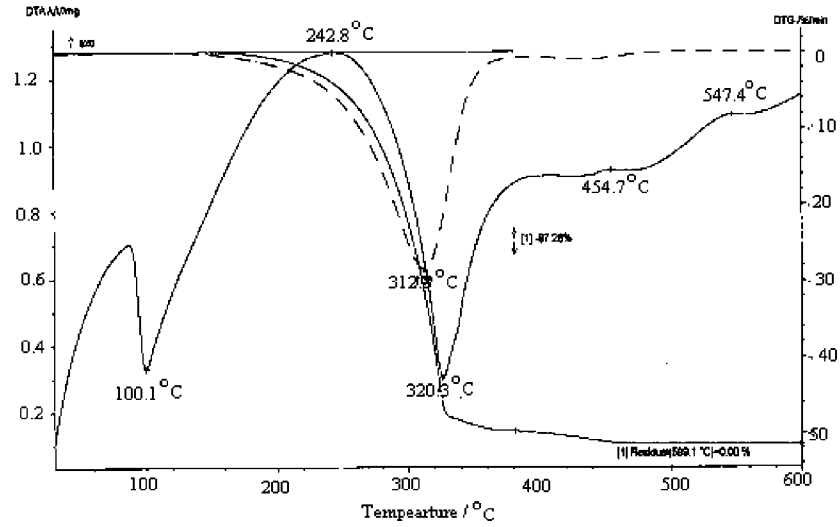

Figure 8. Thermogravimetric analysis spectrum of O-NA doped benzil.

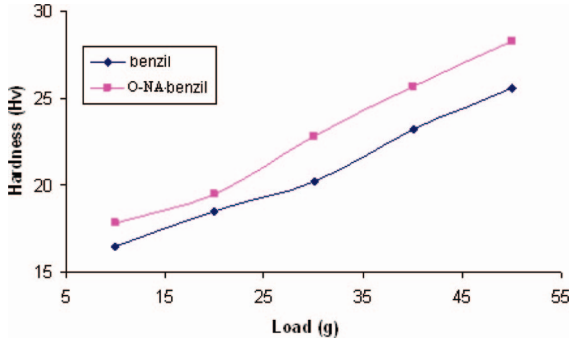

Figure 9. Dependence of Vickers microhardness on load of benzil and O-NA doped.

significant changes in the spectrum of benzil, which could be associated with the weak van der Waals bond; stronger interaction could exist between the guest and the host molecule by the hydrogen bonding. Incorporation of O-NA in the lattice enhances the crystallinity, which is evident from the increase of emission intensity of O-NA doped benzil. The increase in mechanical hardness on O-NA doped benzil may be due to the strong hydrogen bond formed on doping of O-NA. The values of nonlinear refractive index n_2 of benzil and O-NA doped benzil are -9.4×10^{-9} cm^2/W and -6×10^{-7} cm^2 /W, respectively. The values of nonlinear absorption coefficient β of benzil and O-NA doped benzil estimated from the open Z-scan curve are -78×10^{-3} cm/W and -22×10^{-3} cm/W, respectively. FOM values of benzil and O-NA doped benzil are 2265 and 4990, respectively. This implies that the FOM increases on doping of O-NA with benzil, which confirms that the addition of O-NA increases the nonlinearity of the benzil, hence making it highly useful for NLO applications.

Acknowledgment. The authors thank Dr. Shailesh N. Sharma of National Physical Laboratory, New Delhi, India, for helping us in the PL studies.

References

(1) Stanculescu, A.; Antohe, S.; Alexandru, H. V.; Tugulea, L.; Stanculescu, F.; Socol, M. *Synth. Met.* **2004**, *147*, 215.
(2) Sheik-Bahae, M.; Hutchings, D. C.; Hagan, D. J.; Van Stryland, E. W. *IEEE J. Quantum Electron.* **1991**, *27*, 1296.
(3) DeSalvo, R.; Said, A. A.; Hagan, D. J.; Van Stryland, E. W.; Sheik-Bahae, M. *IEEE J. Quantum Electron.* **1996**, *32*, 1324.
(4) Karavanskii, V. A.; Krasovskii, V. I.; Petrov, Y. N.; Zavalin, A. I. *Laser Phys.* **1993**, *3*, 1163.
(5) Mervin, E.; Runner, J. *J. Am. Chem. Soc.* **1952**, *74* (14), 3567.
(6) Rai, R. N.; Varma, K. B. R. *Mater. Lett.* **2001**, *48*, 356.
(7) Vogel, A. I.; Tatchell, A. R.; Furnis, B. S.; Hannaford, A. J.; Smith, P. W. G. *Vogel's Textbook of Practical Organic Chemistry*, 5th ed.; Longman Group UK Ltd.: New York, 1989.
(8) Noginov, M. A.; Curley, M.; Noginova, N.; Wang, W. S.; Aggarwal, M. D. *Appl. Opt.* **1998**, *37*, 24.
(9) Wan, J.; Wang, Z.; Chen, X.; Mu, L.; Yu, W.; Qian, Y. *J. Lumin.* **2006**, *121*, 32.
(10) Tripathy, S.; Soni, R. K.; Asahi, H.; Gonda, S. *Physica B* **2000**, *275* (4), 301.
(11) Gott, J. R. *J. Phys. B: Atom. Molec. Phys.* **1971**, *4*, 116.
(12) Shimoji, N.; Hashimoto, T.; Nasu, H.; Kamiya, K. *J. Non-Cryst. Solids* **2003**, *324*, 50.
(13) Castillo, J.; Kozich, V. P.; Marcano, A. O. *Opt. Lett.* **1994**, *19*, 171.
(14) Sutherland, R. L. *Handbook of Nonlinear Optics*; Marcel Dekker Inc.: New York, 1996.
(15) Sheik Bahae, M.; Said, A. A.; Wei, T. H.; Hagan, D. J.; Stryland, E. W. V. *IEEE J. Quantum Electron.* **1990**, *26*, 760.
(16) Seo, J. T.; Yang, Q.; Creekmore, S.; Tabibi, B.; and Temple, D. *Appl. Phys. Lett.* **2003**, *82* (25), 4444.
(17) Mott, B. W. *Micro-Indentation Hardness Testing*; Butterworths: London, 1956; p 9.

CG701132F